Design of a Scaled Down Acoustic Experiment with Anechoic and Reverberation Chambers

Undergraduate Honors Thesis

Presented in Partial Fulfillment of the Requirements for

Graduation with Distinction in the

Department of Mechanical Engineering at

The Ohio State University

By:

Eric D. Ricciardi

Advisors: R. Singh, Mechanical Engineering, singh.3@osu.edu

J. Dreyer, Mechanical Engineering, dreyer.24@osu.edu

******

The Ohio State University

March 2013

Defense Committee:

Dr. Rajendra Singh

Dr. Jason Dreyer

Dr. Brian Harper

Abstract

The focus on this research is to design and evaluate a split chamber that can be used for measuring random incidence properties of acoustic materials and achieve reliable results for frequencies larger than 500 Hz. A split chamber consists of an anechoic section and a reverberant section; therefore the sound field in each portion must be designed to simulate direct and diffuse field conditions in the far field. The challenge in this test chamber design is adhering to small scale dimension constraints of 2.4m x1.2m x 1.2m and a maximum cost of $1000, while maintaining a certain level of performance in terms of lowest frequency that can be characterized. By analyzing both acoustical field theory and absorption characteristics this chamber is found to have a cutoff frequency of approximately 570 Hz. The far field sound pressure distribution in the reverberant chamber was determined to be sufficiently uniform, both in the room and across the panel. Sound pressure measurements in the anechoic chamber correlated well to the inverse square law, given by ideal direct field conditions. The noise reduction of the room to the outside ranged from 27 dB to 40 dB across the designed frequency range, which indicates that the chamber is sufficiently sealed from the ambient sound. The chamber was built to be within the sizing constraints and met a final construction cost under $1000. This split chamber will be used to assist in student projects and as a teaching tool for mechanical engineering courses. Future work on this project will consider the addition of diffusers in the reverberant chamber; this study will be done using boundary element modeling software and experimental measurements.

Table of Contents

Acknowledgements

I would like to thank all of the individuals that have provided support and guidance over the course of this project. I would like to acknowledge Dr. Rajendra Singh, Dr. Jason Dreyer, and Dr. Brian Harper for their service in my defense committee and the guidance and critique they offered. I would like to thank the Acoustics and Dynamics Laboratory and the Department of Mechanical Engineering at The Ohio State University for the use of their facilities and other resources. Finally, a special thanks to The Undergraduate Honors Committee in the College of Engineering for the financial support awarded during the duration of this project.

List of Figures

Chapter 1: Introduction

1.1 Background

Acoustic materials are used in a wide range of applications in industry, from small scale product design to large scale construction applications. Investigation of acoustic properties is often implemented in the design process of enclosed environments. Generally, objectives of this investigation can fit into one of three classifications: noise control, music perception/enjoyment, or speech intelligibility. Each of these classifications requires a different approach to the design problem and the choice of acoustic treatment. There are a wide range of acoustic properties available on the market and it is valuable to be able to characterize these materials in order select the best material for a given design problem. The acoustic properties of materials to be quantified by this test apparatus are: absorption coefficient (α), transmission loss (TL) and insertion loss (IL). Noise reduction (NR) and sound transmission class (STC) are also often reported but have little scientific meaning. These properties can be measured for a panel of a given material or of an enclosure. For applications involving music perception/enjoyment or speech intelligibility α is the dominating acoustic property. Likewise, for noise reduction applications, TL and IL are the dominating properties to be considered. There are several methods for determining these properties. This research focuses on random sound incidence properties of materials, which requires a split-chamber design to characterize panel treatments.

Acoustic properties of materials can be characterized by using either random sound incidence or normal sound incidence. Figure 1 illustrates normal sound incidence; the initial sound is the sound originating from a sound source, this sound comes in contactwith the solid material at a 90° angle (normal) and is reflected/transmitted in the normal direction. Normal sound incedence test methods include sound only in the normal direction.

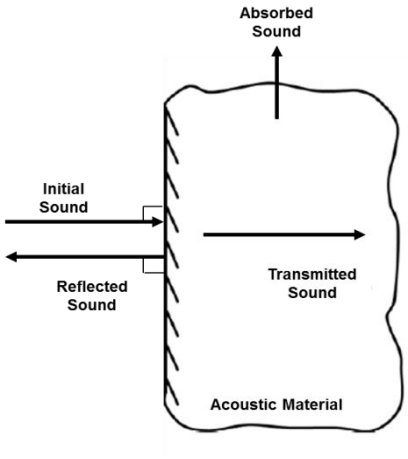

Figure 1: Normal Sound Incidence

However in many real world applications sound approaches at many different angles. Figure 2 illustrates the concept of random sound incedence. The initial sound approaches at various angles and is reflected/transmitted at various angles. Snell's law can be used to describe the relationship between the agnels of incedence and refraction.

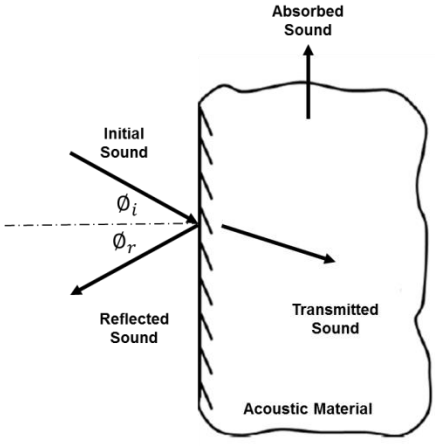

Figure 2: Random Sound Incidence

Bench-top devices, such as impedance tubes, used to characterize acoustic material properties exist, but assume plane waves and are therefore restricted to study normal sound

incidence. Figure 3 illustrates the impedance tube method as defined by ASTM-C384 (American Society for Testing and Materials) [11]. A loud speaker is attached to a standing wave tube and along slender probe is used to identify nodes/antinodes in the standing wave and this data can be used to find the normal absorption coefficient α_n shown in Equation 1, where n is the ratio of maximum sound pressure to adjacent minimum.

$$\alpha_n = \frac{4}{n+\left(\frac{1}{n}\right)+2} \qquad (1)$$

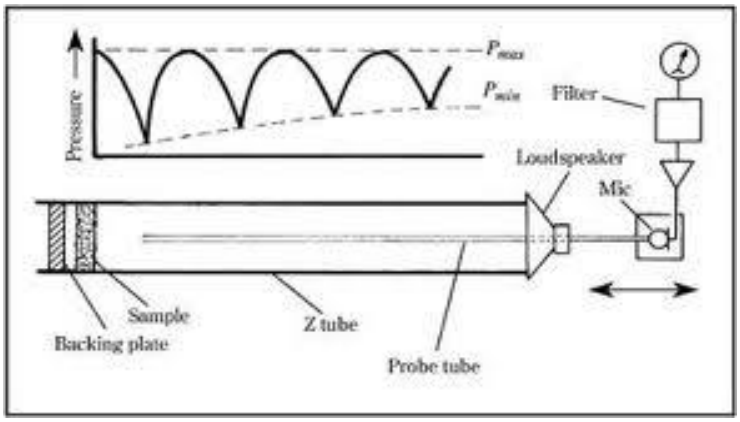

Figure 3: Impedance Tube Method [11]

Normal incidence properties are valuable for applications in duct acoustics such as mufflers, plumbing, etc. However, in many real environments, such as vehicle cabs and concert halls, this plane wave assumption is poor when used to predict the sound fields. A random sound incidence is often a more realistic condition. In order to measure acoustic properties subjected to random sound incidence, a large room, rather than a tube, must be used. A spit chamber design with adjoining anechoic and reverberant sides is often employed for this type of testing as outlined in ASTM standards E90 and C423.

1.2 Significance of Research

The Acoustic and Dynamics Laboratory (ADL) at The Ohio State University currently has a working test set-up for characterizing normal incidence properties of acoustic materials, but there exists no such set-up for random sound incidence; any such testing must be done in an outside laboratory. As previously noted, there is significant real world application for random incidence properties and this project will provide the means to test these properties. The split-chamber constructed and evaluated as a result of this project can be used for industry sponsored projects as well as a valuable teaching tool for undergraduate and graduate students. This split-chamber will possibly be used for laboratory experiments in acoustics courses offered through the Mechanical Engineering Department.

The applications of random sound incidence are mostly for studying the effects of panel treatments in different rooms; lecture halls, concert halls, recording studios, etc. When considering acoustics in the design of a room, it is also valuable to be able to characterize the sound field within that room. Characterization of a room includes estimating *direct field* and *diffuse field* contributions; which involves quantifying how much of the sound you are hearing is directly from the sound source (*direct field*) and how much has been reflected from a surface within the room (*diffuse field*). Often, these field contributions are estimated during the design process and evaluated after construction. The split-chamber design considered in this project includes a completely anechoic room (*direct field*) and a completely reverberant room (*diffuse field*). In order to design/evaluate this split-chamber the fields in each room must be characterized with a similar method used in real world construction applications.

1.3 Project Formulation and Scope

The main deliverable of this research is to develop a small-scale acoustic test chamber (spit chamber design) that can be used to characterize acoustic properties of panel treatments subjected to random sound incidence. ASTM standards E90 [2] and C423 [3] will be used as references to construction and testing procedures. Those standards describe the type of enclosure and test method used to characterize random incidence properties of materials. ASTM E90 and C423 refer to the "Standard Test Method for Laboratory Measurement of Airborne Sound Transmission Loss of Building Partitions and Elements" and the "Standard Test Method for Sound Absorption and Sound Absorption coefficient by the Reverberation Room Method" respectively. The objectives of this project are:

i) Design of small scale split-chamber and determination of materials needed.

ii) Fabrication of the design.

iii) Evaluation of test chamber and report of cutoff frequency (lowest reliable frequency for measurements).

This project should yield a working chamber with a defined test method to measure *IL*, *TL* and α. This chamber should be useful for frequencies above 500 Hz, the actual value of the chamber will be measured. The scope of this project requires both computational and experimental components. Transmission phenomena will be studied in the calculation and measurements of α, and one for *TL* and *IL*. Acoustic field theory will be used to characterize the field within the anechoic and reverberant rooms. Experimental results will be compared to the theoretical calculations for transmission phenomenon and acoustic field theory. This project will conclude with suggestions for improvements on the design and further study using this split-chamber.

Chapter 2: Design/Fabrication

2.1 Design Considerations/Constraints

The major challenge in the design of this split-chamber is to adhere to ASTM standards as closely as possible while adhering to sizing and budget constraints. ASTM E90 describes standards for the construction of such a chamber [2]. These chambers are reliable for frequencies above 200 Hz and are generally 125 to 300 m^3 in volume, and require a sample size of 1 m^2; these chambers can cost hundreds of thousands of dollars. Figure 4 shows an example of a full scale split chamber design built by ETS-Lindgren [10].

Figure 4: Example of Full Scale Split-Chamber [10]

This device designed in for this project should serve as a bench top test chamber with approximate dimensions of 1.8 m by 1.2 m footprint with 1.8 m height. The cost of the chamber is also not to exceed $1000 in materials. The chambers must provide some access to the sample panels as well as the microphones. A sample size of 1/4 m^2 will be used. Construction of the chambers will require proper sealing of the joints as well as material selection for the partition

materials, such as medium density particle board, in order to reduce unmeasured transmitted sound into or out of the chambers.

Reverberation chamber sizes defined in the ASTM specifications are a minimum of 125 m^3 in volume. The volume and length requirements of the chamber is recommended to be greater than $4\lambda^3$ and a major dimension greater than 1.5λ, where λ is the wavelength in m of the lowest frequency in Hz of interest to be measured. Reverberant chambers are usually constructed from hard rigid walls to reflect virtually all of the sound. The challenge in designing and building a reverberant chamber is to reduce break up enclosure modes, also referred to as standing waves. Many different physical apparatuses can be used to minimize standing waves such as: diffusers, large rotation reflective vones (a fan like object), and warble tones or random noise generators [4]. In addition, the walls of these chambers are often constructed at different adjoining angles to reduce parallel and perpendicular surfaces. The crucial feature of a reverberant chamber is that the sound pressure level readings are uniform throughout the chamber; this will be observed so long as there are minimal standing waves. Measurement techniques often include multiple microphones placed at different locations within the chamber or a single microphone may be placed on a rotating boom and the measurement becomes spatially averaged as the traveling microphone data is time averaged.

Anechoic chambers are designed to accommodate the maximum absorptive treatment while still allowing for a sample to be placed within the chamber. In the case of panel characterization, almost all of the volume reserved for the anechoic chamber can be devoted to absorptive materials as the panel will only be placed on the wall adjoining the two chambers. This is an effective design as long as the wall treatments do not interact with the panel sample. The lowest effective frequency for the anechoic chambers is often dictated by the thickness of

the wall/floor/ceiling treatments, typically composed of porous foam wedges. Wedge or cone shapes are often used in order to treat multiple sound incidences within the room. The depth or thickness of the treatment should be greater than $1/4\lambda$ of the lowest frequency measured. An example of these wedges can be seen in Figure 5. Testing set-ups include multiple microphones directed at the surface of the panel; microphones may also be placed near the wall and spatially averaged to reduce testing variability. The majority of the material cost will rest on the anechoic treatment material.

Figure 5: Anechoic Room [10]

The major dimensions of the chambers will designed using sizing considerations described above. The placement of the microphones and diffusers in the reverberation chamber will be determined via field theory calculations and experimental measurements. Different acoustic treatment material properties, required to determine the maximum performance of the anechoic chamber in terms of background level and desired free sound field , will be selected

from catalog values, but will their performance will be quantified with measured valued after mounted.

2.2 Proposed design

The size needed for each chamber can de deterimend by considering sizing equations discussed in Section 2.1 and the desiered cutoff frqeuncy of 500 Hz. After considering the constraints of this project and the designs specified by ASTM a SolidWorks model was built to esnure the design's viability. Part drawings for the chosen parts were imported from McMaster-Carr [13]. Figure 6 shows a wireframe model of the entire split chamber design.

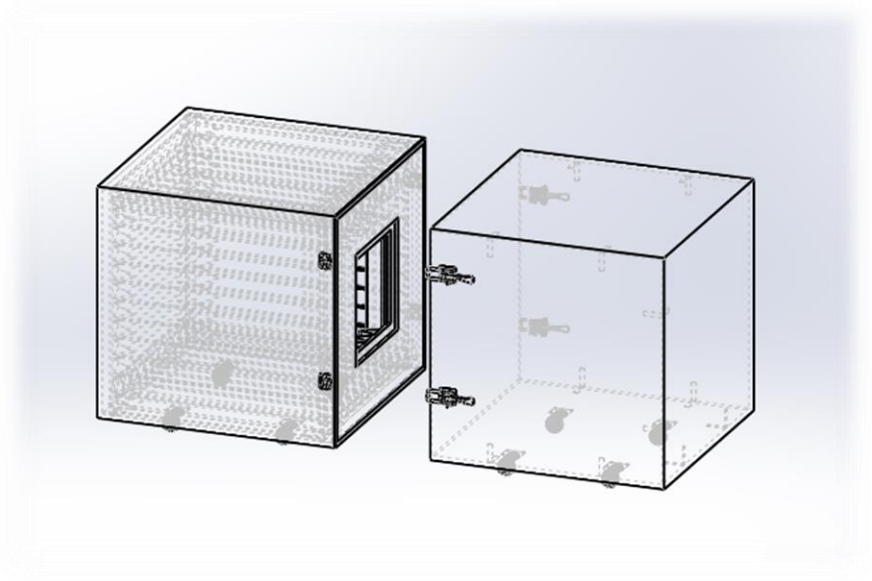

Figure 6: Wireframe Solidworks Model

Figures 7 and 8 show the anechoic and reverberant chambers (respectively) and the part descriptions for each chamber, dimensions are noted in English units per manufacturer specs. The frame designs for both sides are essentially the same, with alterations for the acoustic side to include foam treatment and sample mounting. MDF (Medium Density Fiberboard) was chosen

because of its high density and rigid properties. The estimated cost of this design is $850 which fits within the budgetary requirements.

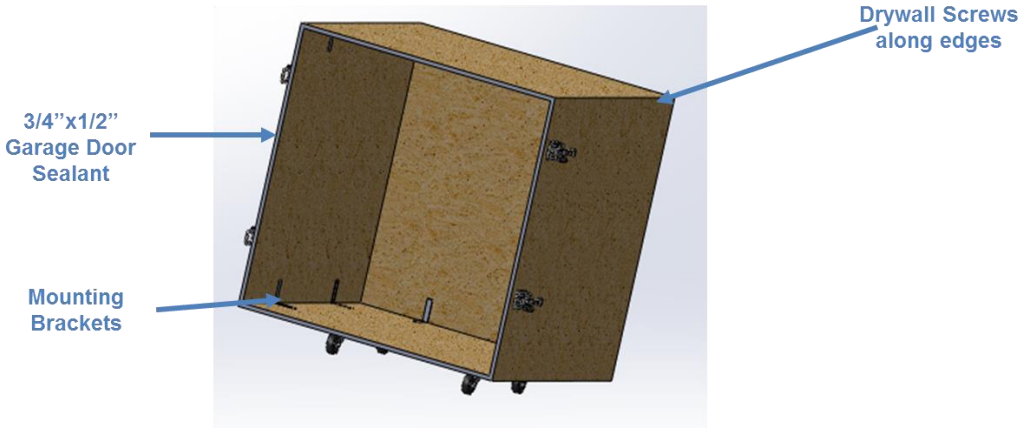

Figure 7: Reverberant Chamber Design

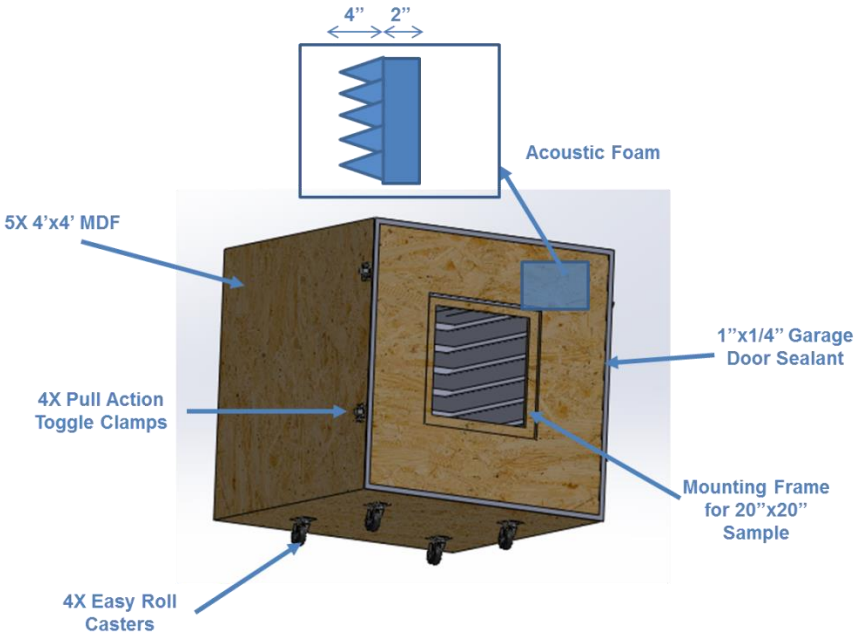

Figure 8: Anechoic Chamber Design

2.4 Construction

Figure 9 shows the four casters being installed to the base plate with through bolts and Figure 10 shows the construction of the main frame; this was done by using brackets to attach the MDF panels to the base board. Eight drywall screws were then installed on each edge for added stability. This process was used for both anechoic and reverberant chambers.

Figure 9: Installing Casters

Figure 10: Building Frame

Once construction of the frame was completed each edge was sealed by using caulking, as shown in Figure 11. The clamps were then lined up and installed on each side and the sealant was stapled into place on the connections between the two sides, as shown by Figure 12.

Figure 11: Caulking the Seems

Figure 12: Sealant and Clamps

Figures 13 and 14 show the final mounting for the test panel, three blocks were installed to hold the sample in place.

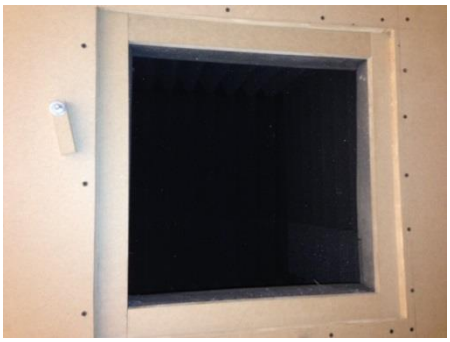

Figure 14: Installing Sample Mount

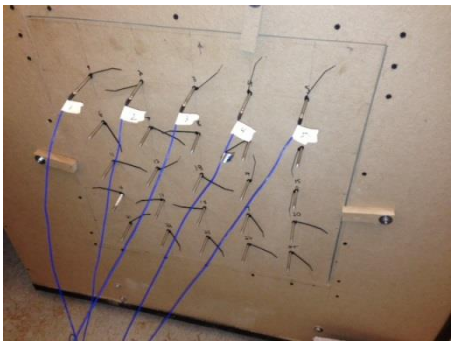

Figure 13: Mounted Panel (25 Mic Array)

Figures 15 and 16 depict the process of installing the foam. First the flat foam was adhered to the frame using foam adhesive. The wedges were then adhered to the flat foam with the same adhesive. This adhesive took an hour to set so supports had to be used during this time.

Figure 16: Foam Wedges

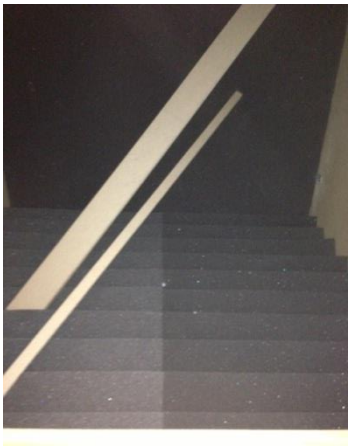

Figure 15: Installing Foam

2.6 Final Chamber

The major change in the design was the type of clamp used to connect the two rooms. After initially trying a smaller clamp a larger one had to be ordered because the smaller clamps were not strong enough and pulled out of their fixture. It was also decided to initially test the reverberation chamber without diffusers to see if they were needed in order to achieve a more diffuse field. Figures 17-20 show images of the final chamber.

Figure 18: Both Chambers (Open)

Figure 17: Reverberation Chamber

Figure 20: Anechoic Chamber

Figure 19: Inside of Anechoic Chamber

Chapter 3: Theoretical Considerations

3.1 Direct and Diffuse Field Theory

As stated in Section 1.1, every sound field has some contributions from the direct field and diffuse field. The objective for this split chamber design is to have a chamber with an entirely diffuse field and a chamber with an entirely direct field. However, due to sizing constraints, this design will not be able to achieve these perfect field conditions.

In a diffuse field the sound pressure is the same at every position in the far field; far field assumptions excludes positions close to the walls and close to the source (defined as one major dimension from the source). This assumes that all the boundary conditions are ridged, i.e. velocity release surface; and that there is no absorption in the room. Therefore if a sound source exists within the room no energy will ever be dissipated and the energy density in the room (ε_d) will continue to rise and approach an infinite number of modes. This phenomenon is known as the "cocktail party effect". [6] The analogy is to a room of individuals that continue to speak louder which causes other to speak louder; eventually speech is entirely intelligible and the sound pressure in the room is so high no one can understand each other. Also, this room would have an infinite reverberation time. Reverberation (T_{60}) time is defined as the time it takes for the sound pressure in the room to decrease by 60 dB after a source is shut off as shown in Figure 21. [7]

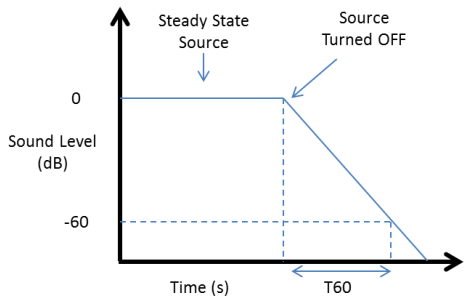

Figure 21: Definition of Reverberation Time

However, it is not possible to have such a phenomenon occur. This effect could only occur in a perfect vacuum since air has absorptive properties; since sound needs a medium in order to propagate it is not possible to observe this phenomenon. A well-built reverberation chamber will have reverberation times upwards of 8 seconds [12]. It is often not possible to observe a 60 dB reduction in the room so reverberation time can be calculated in other manors, described later, or can be defined for another increment of dB reduction i.e. T_{40}.

Direct field theory is quite opposite to diffuse field theory; in a perfect direct field reverberation time would be 0 seconds. In a direct field there are absolutely no reflections from the boundaries. To understand this concept it is helpful to understand the concept of acoustical impedance. Specific acoustical impedance is given by Equation 2, where p is the sound pressure and u is the particle velocity. For anechoic termination at boundary conditions specific impedance of the boundary (frequency dependent) must equal the impedance in air time the particle velocity, shown by Equation 3.

$$z = \frac{p}{u} \quad [\frac{Ns}{m^3}] \tag{2}$$

$$\widetilde{z_s} \rightarrow z_o u \quad [\frac{Ns}{m^3}] \tag{3}$$

The pressure distribution in a direct field is not uniform; it is related by the inverse square law as shown in Equation 4 (not valid near the source). As a result of this distribution a doubling of distance from the source will result in -6 dB change in sound pressure.

$$L_p \sim \frac{\Gamma}{4\pi r^2} \text{ [dB]} \qquad (4)$$

Both direct and diffuse field theories assume that there is no outside noise leaking into the room. They also assume a simple lumped theory approach applied to room acoustics.

3.2 Room Modes

The previous section assumed a simple lumped approach; however, there are two more commonly used theories in room acoustics: ray tracing and wave theory. In this section ray tracing theory will be utilized to analyze normal room modes of an enclosure. The enclosure being analyzed is the reverberation room; ray tracing would not be applicable to the anechoic chamber because to rays would be reflected. The purpose of this analysis is to ensure a uniform pressure distribution in the room and across the test panel. Figure 22 illustrates the path of a single ray being traced from the source and reflected against the rigid walls of the enclosure. [5]

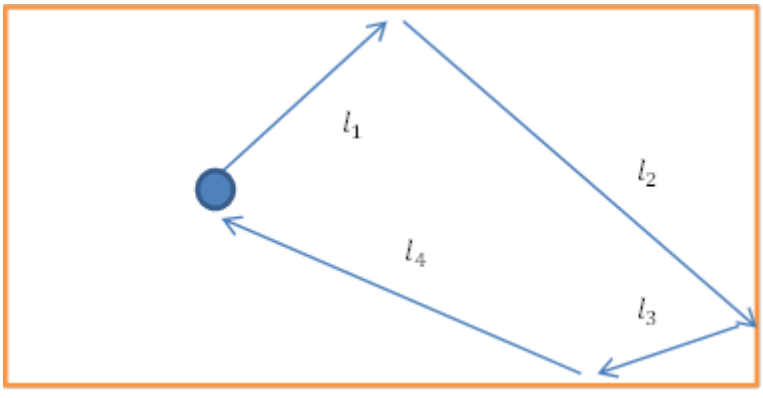

Figure 22: An Example of Ray Tracing from the Source

If the total length traveled by a ray is an integer multiple then a normal mode frequency is reached, shown by Equations 5 and 6. Equation 7 gives us the frequency in Hz of this mode for a 2D case. [5]

$$l = l_1 + l_2 + l_3 + l_4 \text{ [m]} \quad (5)$$

$$n\lambda = l \text{ [m]} \quad (6)$$

$$f_n = nc_o/l \text{ [Hz]} \quad (7)$$

$$n = 0,1,2,3 \ldots \infty$$

Equation 8 gives us normal modes with a 3D hard walled enclosure. For a uniform pressure field we want many normal modes as possible; a single mode created by a pure tone will result in uneven pressure distribution. This pressure distribution is given by Equation 9.

$$f_n = \frac{c}{2}\sqrt{(\frac{n_x}{l_x})^2 + (\frac{n_y}{l_y})^2 + (\frac{n_z}{l_z})^2} \text{ [Hz]} \quad (8)$$

$$p \propto \sum_{n_x=0}^{\infty}\sum_{n_y=0}^{\infty}\sum_{n_z=0}^{\infty} A_{lmn}\cos(\frac{n_x\pi x}{l_x})\cos(\frac{n_y\pi y}{l_y})\cos(\frac{n_z\pi z}{l_z})\text{[Pa]} \quad (9)$$

$$n_x, n_y, n_z = 0,1,2, \ldots \infty$$

At corners of the room all cosine terms above are equal to one so pressure is given by Equation 10. At the corners, the sound pressure is maximized, so a speaker placed there will have the potential to excite the largest number of modes. Figure 23 and Equation 11 also describe the distribution across the outer wall and more specifically the sample panel.

$$p \propto \sum_{n_x=0}^{\infty}\sum_{n_y=0}^{\infty}\sum_{n_z=0}^{\infty} A_{lmn} \text{ Pa]} \quad (10)$$

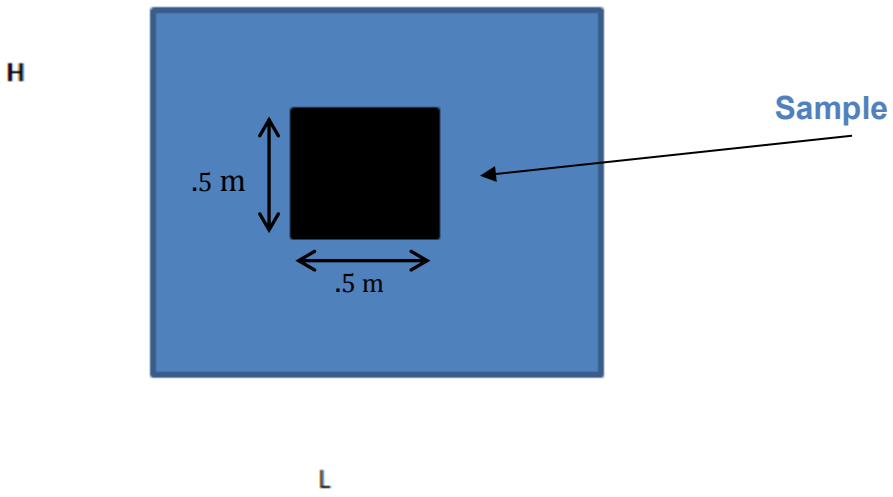

Figure 23: Schematic of Outer Wall With Panel

$$p(x,y) = \sin(\frac{n_x \pi x}{l_x}) \sin(\frac{n_y \pi y}{l_y}) \text{ [Pa]} \quad \textbf{(11)}$$

For purposes of designing this chamber we are mostly concerned with achieve a large number of modes. Equations 12 and 13 give us a relation for the number of modes N in a given room. Equation 12 is for narrow band results and Equation 13 is applicable to band widths; where f is the center frequency and $l_x, l_y,$ and l_z are the major dimensions of the room.

$$N = \frac{4\pi f^3 V}{3c^3} + \frac{\pi f^2 A}{4c^2} + \frac{fL}{8c} \quad \textbf{(12)}$$

$$\Delta N = [\frac{4\pi f^2 V}{3c^3} + \frac{\pi f A}{4c^2} + \frac{L}{8c}]\Delta f \quad \textbf{(13)}$$

$$V = l_x l_y l_z \ [m^3]$$

$$A = 2(l_x l_y + l_y l_z + l_x l_z) \ [m^2]$$

$$L = 4(l_x + l_y + l_z)[m]$$

Figure 24 is a plot of the number of room modes versus frequency. At high frequencies there are a very large number of room modes; however, we are mostly considered with low frequencies. Specifically out target cutoff frequency. The figure also shows a zoomed in portion

of the plot at the cutoff frequency. At 500 Hz (target cutoff) there are only 40 room modes. This could cause an issue for uniform pressure distribution at low frequencies. This theory will be explored experimentally in a later section.

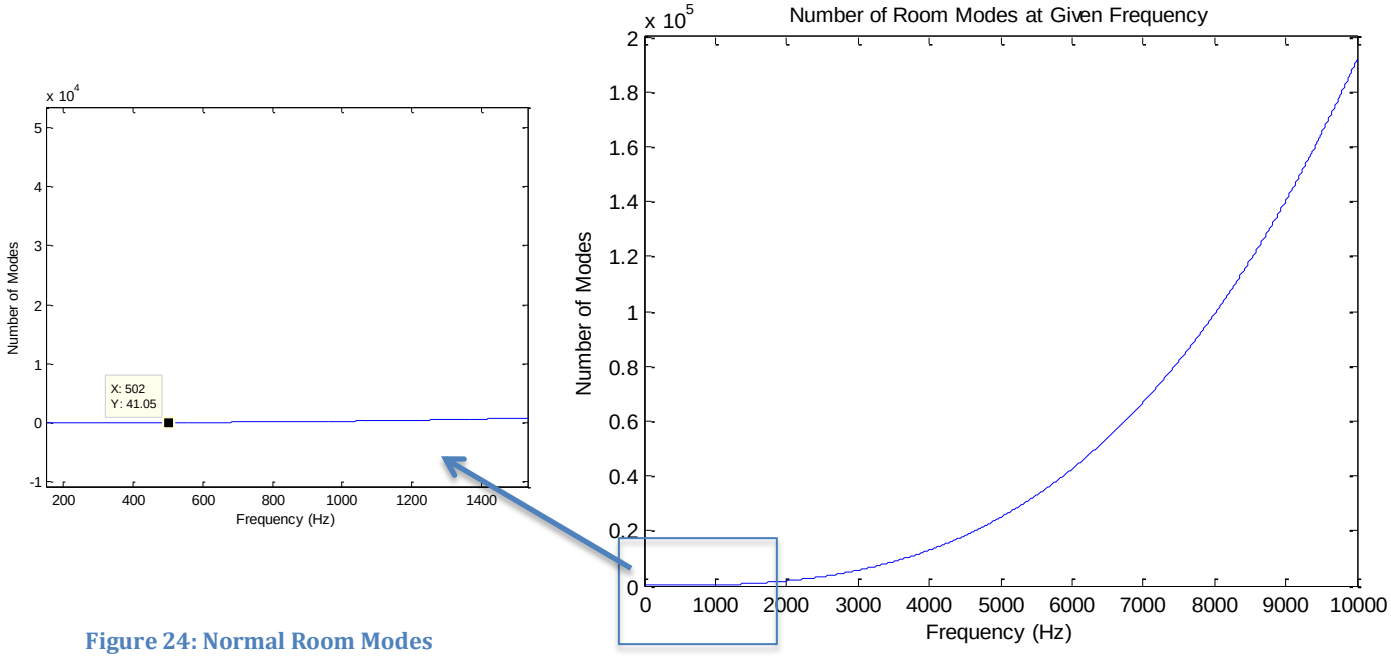

Figure 24: Normal Room Modes

3.3 Surface Interaction (Absorption)

Recall from Figure 1 that when incident sound comes in contact with a surface some of that sound is reflected back, some is transmitted, and some is absorbed. This section is considered with the sound that is absorbed and how α is determined.

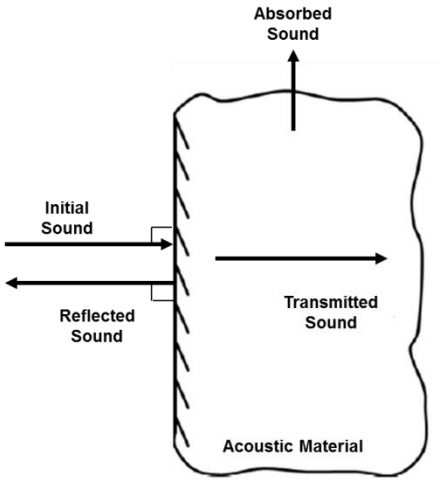

Figure 1

There are many factors that affect the absorptivity of a material: porosity, flow resistivity, and a structure factor. In order to achieve prefect absorption the impedance of the material at a given frequency must match that of the air. And in any room, there are likely many different absorbing materials in a room, which is why we define an average absorption constant $\overline{\alpha}$. The average absorption coefficient $\bar{\alpha}$ can be determined by the summation of the absorption of each material and its respective surface area and dividing by the total surface area S as given by Equation 14. Figure 25 shows some practical values of $\bar{\alpha}$. [6]

$$\bar{\alpha}(\omega) = \frac{\sum \alpha_i(\omega) S_i}{S} \qquad \textbf{(14)}$$

Rough ᾱ values	
ᾱ=0.99	virtually anechoic
ᾱ=0.5	"dead" room
ᾱ=0.1	"medium live" room
ᾱ=0.01	"very live" room

Figure 25: Practical Average Absorption Values

We also define a room constant R as the total absorption power; the effective surface area in the room with perfect absorption.

$$R(\omega) = \bar{\alpha}(\omega)S\ [m^2 - sabine's] \quad \textbf{(15)}$$

Many publications define R defiantly as shown in Equation 16. This equation is generally used for realistic rooms and for diffuse fields whereas Equation 15 would be more applicable to direct fields. This value is defined as R' and is generally used by architects and structural engineers.

$$R'(\omega) = \frac{\bar{\alpha}(\omega)S}{1-\bar{\alpha}}\ [m^2 - sabine's] \quad \textbf{(16)}$$

This R value can also be experimentally determined by using Equation 17. This R value can then be used to calculate $\bar{\alpha}$ from Equation 15 or 16. This procedure will be utilized later for experimental evaluation both chambers.

$$L_p = L_w + 10Log_{10}(\frac{\Gamma}{4\pi r^2} + \frac{4}{R})\ [\text{dB}] \quad \textbf{(17)}$$

Where L_p is a measured value, L_w is of a known power source, $\frac{\Gamma}{4\pi r^2}$ is the contribution from direct field, Γ=1 for spherical radiation; 2 for hemispherical radiation, and $\frac{4}{\text{R}}$ is the contribution from the diffuse field. R can also be used to find reverberation time from Equation 18 and then the cutoff frequency using Equation 19.

$$T_{60} = \frac{55.3V}{Rc_o}\ [\text{s}] \quad \textbf{(18)}$$

$$f_c = 11{,}885\sqrt{\frac{T_{60}}{V}}\ [\text{Hz}] \quad \textbf{(19)}$$

3.4 Surface Interaction (Transmission)

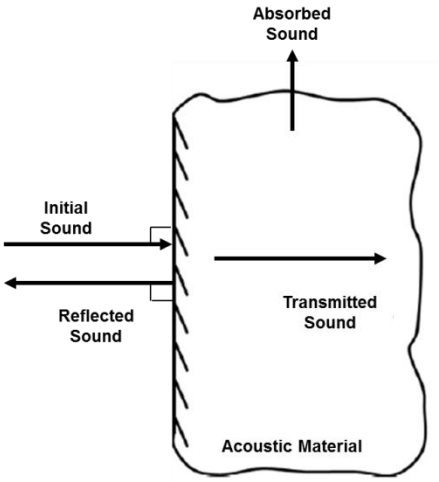

Figure 1

Again, recalling Figure 1, when incident sound come in contact with a surface some of that sound is transmitted through the material. There exist a few different ways of characterizing this effect: *TL*, *IL*, and *NR*. *TL* is the most "scientific" of these measurements and the other two are usually used in construction applications. [6] Transmission loss is a log ratio of the incident sound intensity and transmitted sound intensity, given by Equation 20. Insertion loss is simply the sound pressure (dB) at the receiver with material less the sound pressure without material, given by Equation 21. Noise reduction is defined as the difference between initial sound pressure (measured in the room with the source) and the transmitted sound pressure, given by Equation 22.

$$TL = 10\log_{10}\left(\frac{I_i}{I_t}\right)\ [dB] \qquad \textbf{(20)}$$

$$IL = (L_P - L_{Pt)}\ [dB] \qquad \textbf{(21)}$$

$$NR = (L_{Pi} - L_{Pt}\ )\ [dB] \qquad \textbf{(22)}$$

3.5 Evaluation Criterion

Information from sections 3.1-3.3 will be used in the evaluation of the split-chamber and there are a few key values to report regarding the performance of this test chamber. Recall Equation 19, reporting the cutoff frequency is very important in the evaluation of the test chamber. The reverberation time of the anechoic chamber will give us the cutoff frequency and hence the cutoff frequency of the test set up. Variance V_n^2 or standard deviation V_n can also be calculated using Equation 23 where B is the bandwidth. [1]

$$f_c = 11{,}885\sqrt{\frac{T_{60}}{V}}\ [\text{Hz}] \quad \textbf{(19)}$$

$$V_n^2 = (1 + \frac{BT_{60}}{6.9})^{-1} \quad \textbf{(23)}$$

The variance can then be used to report the minimum number of data points needed (N) when taking measurements using Equation 24. Where e is the allowable sampling error and 2.5 is a constant chosen for 98.75% certainty. For example is +/- 1dB is required that would result in an e value of .259. [1]

$$N \geq (\frac{2.5V_n}{e})^2 \quad \textbf{(24)}$$

3.5 IL, TL, α Test Method

Figures 26 and 27 test methods for determining TL, IL and α using the split chamber test set up. These methods are described in ASTM standards and have been adapted to this project.

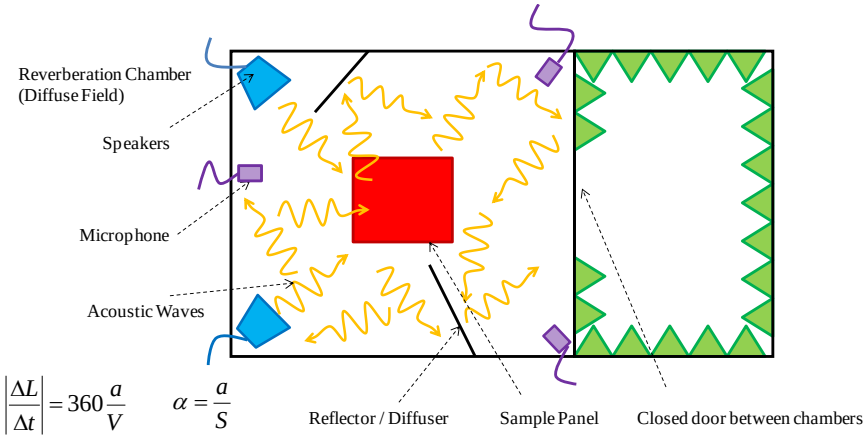

Figure 26: Absorption Test Method

Figure 26 shows a schematic of split test chamber for sound absorption characterization of panel treatments (reverberation chamber side only), where *a* is sound absorption in m^3, $\Delta L/\Delta t$ is sound pressure level decay rate in dB ref 20 μPa/s, and *V* is volume of the room in m^3, and *S* is the exposed surface area of the treatment in m^2. This method was not used to calculate average absorption in the chamber but can be used to determine properties of sample panels.

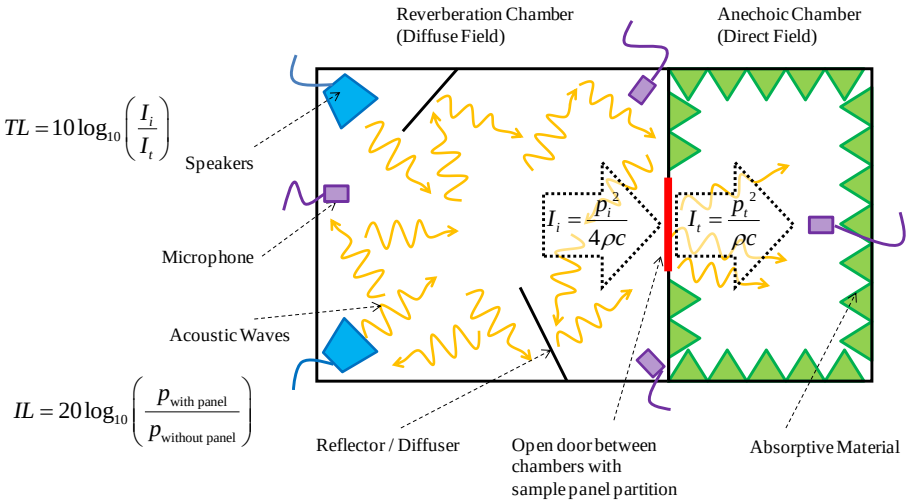

Figure 27: TL and IL Test Method

Figure 27 shows a schematic of split test chamber for insertion loss (IL) and transmission loss (TL) characterization of panel treatments. I_i is the incident sound intensity, I_t is the transmitted sound intensity, p_i is the spatially averaged incident *Prms*, p_t is the spatially averaged transmitted *Prms*.

Chapter 4: Experimental Evaluation

4.1 Testing Set-Ups

A variety of test set-ups were used in the evaluation of this design. In each test set up background noise data was collected to ensure results were more than 10 dB above background noise to avoid any need for background correction. Also, all sound pressure data collected was rms data given by Equations 25 and 26.

$$< P_{rms}^2 >_t = \frac{1}{2\tau}\int_{-\tau}^{\tau} P^2(t)dt \qquad \textbf{(25)}$$

P_{rms}=Sound Pressure Data Collected

$$P_{ref} = 20\mu Pa$$

$$L_p = 20\log(\frac{P_{rms}}{P_{ref}}) \text{ [dB]} \qquad \textbf{(26)}$$

The first set up was using a known power source to measure $R(\omega), \bar{\alpha}(\omega)$, and T_{60} for both chambers and to determine the cutoff frequency of the anechoic chamber. The power source, shown in mounted in Figure 28, was manufactured by ILG Industries. It is essentially a fan than produces a known power level at given frequencies. [9] The mounting shown in Figure 28 is assumed to hemi-spherical (defined by equation 17).

Figure 28: Mounted Power Source

Three microphones were placed in the anechoic room, shown in Figure 30, at distances .3, .61 and .83 meters away from the source along an orthogonal path to the source; there was also a microphone placed outside of the room on the lab bench shown in Figure 29. to collect ambient sound. The known sound power source was mounted and the room was sealed before data collection, shown in Figure 29. This process was repeated for the reverberant chamber; however, a vibration dampener was placed underneath the microphone stand to isolate and structure born noise that could occur, shown in Figure 31.

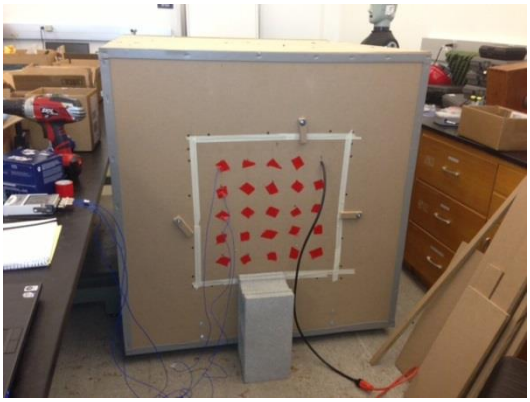

Figure 29: Sealed Anechoic Chamber

Figure 30: Anechoic Microphone Set-up

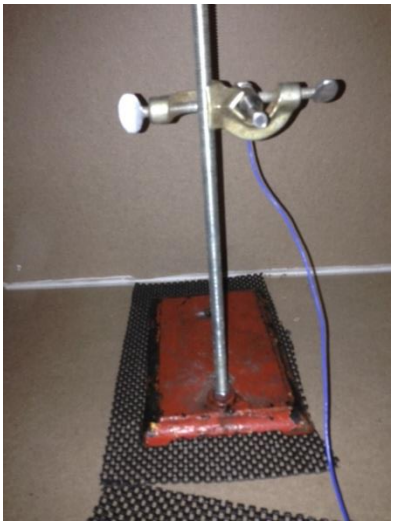

Figure 31: Vibration Idolaters

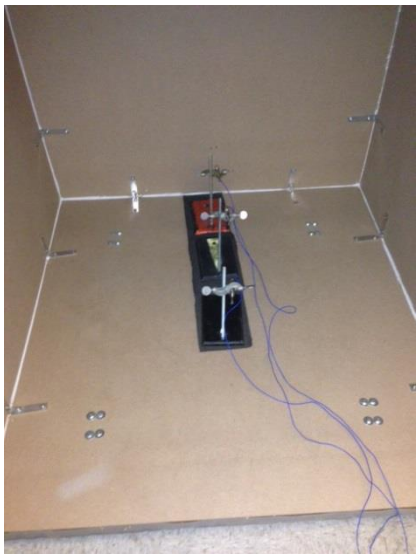

Figure 32: Reverberation Chamber Microphone Set-up

The next test set-up was used to evaluate the uniform pressure distribution in the reverberant chamber to see if any diffusers were needed in the design. This testing was done in the anechoic side before any acoustic treatment was applied in order to take advantage of the sealed room. First a 25 microphone array was used in place of a sample panel to ensure a uniform pressure distribution across the panel, shown in Figure 34. Two speakers were placed in the chamber pointing at corners, to excite as many modes as possible, and they produced white noise at 3V p-p, shown in Figure 33. This process was repeated but microphones were placed at 11 various locations in the room as defined by Figures 35 and 36.

Figure 33: Speaker Set-Up

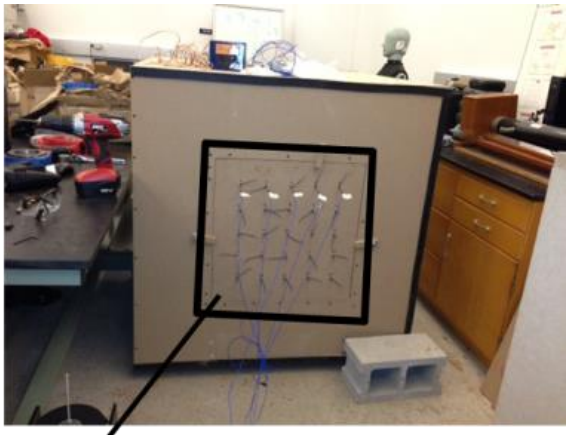

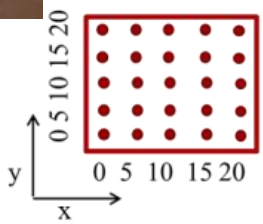

Figure 34: Microphone Array

Mic Placement		
x (m)	y (m)	z (m)
0.46	0.30	0.46
0.76	0.30	0.46
0.46	0.61	0.46
0.76	0.61	0.46
0.46	0.91	0.46
0.76	0.91	0.46
0.46	0.30	0.91
0.76	0.30	0.91
0.46	0.61	0.91
0.76	0.61	0.91
0.46	0.91	0.91

Figure 36: Microphone Placement

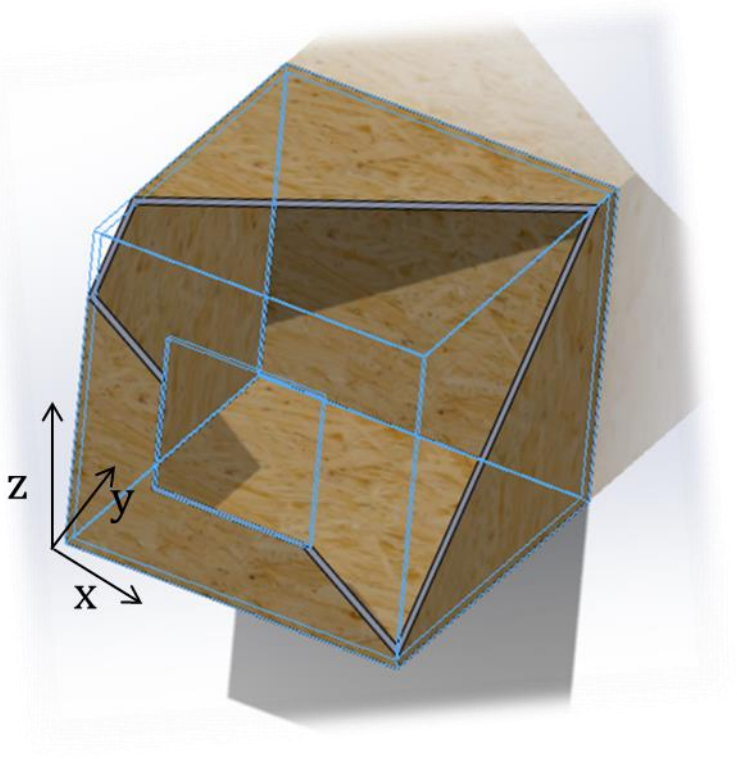

Figure 35: Coordinate Definition

The final testing done was to find values for *TL*, *IL*, and *NR*. These values were found for the .25x.25 m panel of MDF and also for varying percentages of openings in the panel, air gaps. The same sound source set up was used for the previous procedure and microphones were placed in both the anechoic and reverberant chambers. The same procedure present by Figure 27 was followed for this experiment. The procedure was repeated for: an intact panel, .1% air, .15% air, 2% air, and no panel (17% air). Figure 37 shows a panel with a hole resulting in a .1% air gap.

Figure 37: Panel with ¾" Diameter Air Gap

4.2 Cutoff Frequency and Absorption Measurements

Figure 38 shows the background noise measurements at 1/3 octave bands. These values are less than 10 dB for the rest of the measurements with the source turned on therefore no correction for background noise is needed.

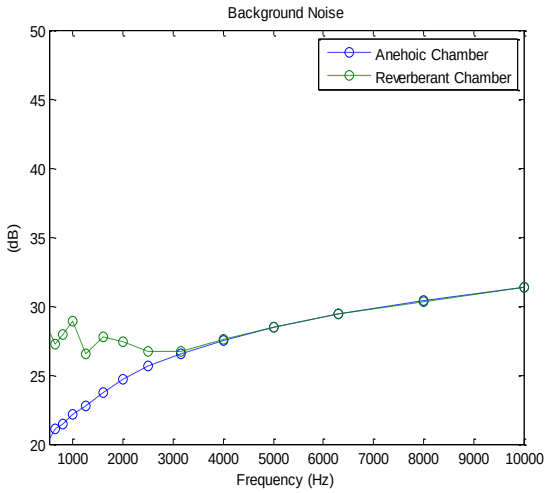

Figure 38: Background Noise

Figures 39 and 40 show sound pressure (Lp) data for 1/3 octave bands at varying distances of *r* (in m). Circular markers are used in plotting to illustrate the variance of measured values. The origin of each circle is the precise measured value and the radius of the circle indicates a +/- 1 dB range. As expected results for the reverberant chamber look fairly uniform and the results for the anechoic chamber seem to follow the inverse square law. To analyze this further the sound pressure data at a chosen frequency (1250 Hz) was plotted versus the distance from source, this data is shown in Figures 41 and 42. Again, values for the reverberant chamber are uniform as expected and the slope of the anechoic plot is approximately -5.7 dB/octave which is similar to the theoretical value of -6 dB/octave but can only be reported with+/- 1 dB accuracy. dB/octave refers to the sound pressure level loss by double the distance from a source.

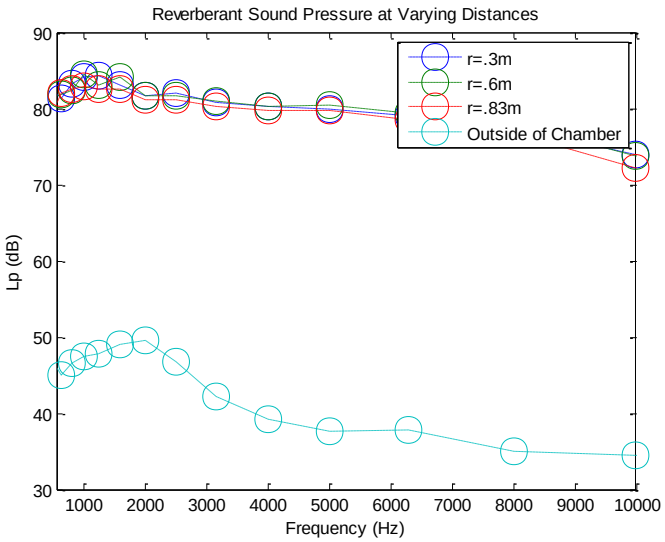

Figure 39: 1/3 Octave Band Spectrum for Reverberant Chamber at Varying Distances r

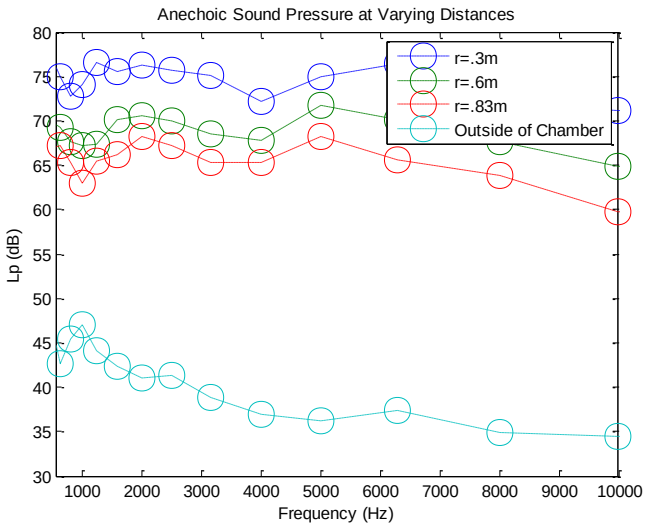

Figure 40: 1/3 Octave Band Spectrum for Anechoic Chamber at Varying Distances r

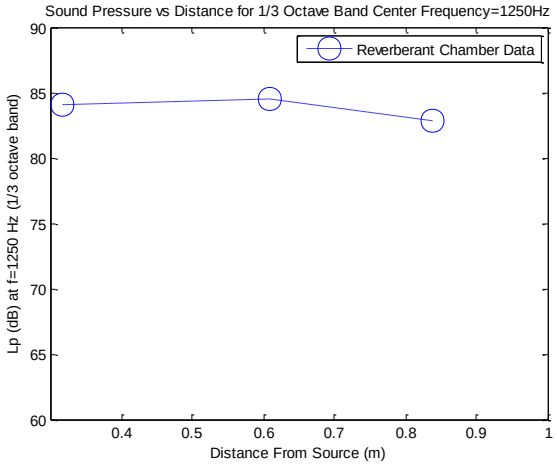

Figure 42: Reverberant Lp vs Distance From Source

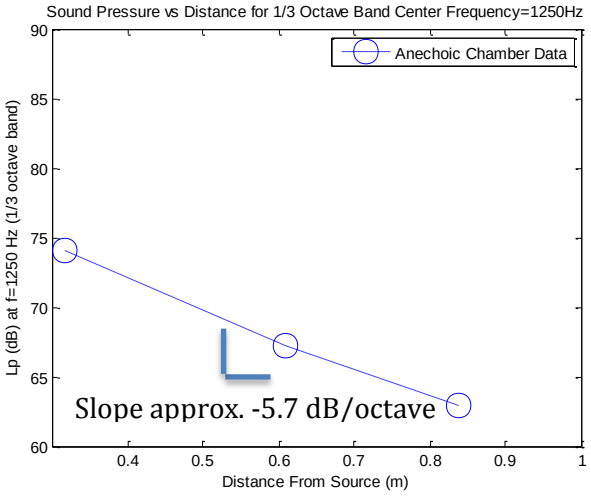

Figure 41: Anechoic Lp vs Distance From Source

This test set up was also used to find value for $R(\omega), \bar{\alpha}(\omega),$ & T_{60} for each room at 1/3 octave bands. It was chosen to report from 630 Hz to 2500 Hz because the ASTM standards report 1/3 octave band data similarly. Figures 43 and 44 show this data. Values for $\bar{\alpha}(\omega)$ should be as close to 1 as possible and values for this chamber range from .78 to .92; these values are

very good for a room of this size. The cutoff frequency was arithmetically averaged and came out to be 67 Hz higher than what was designed for. Values for the reverberant chamber are actually quite pleasing. Absorption ranges from .05-.09 which is very good for a room this size; recall values of .01 indicate a very "live" room.

Figure 43: Table of Values for Anechoic Chamber

Anechoic Chamber								
Center Frequency 1/3 Octave Bands (Hz)								
	630	800	1000	1250	1600	2000	2500	Average
R(ω) [m^2]	41	38	43	48	57	18	26	/
ᾱ(ω)	0.891	0.883	0.896	0.906	0.920	0.785	0.839	/
T60 [seconds]	0.004	0.004	0.004	0.003	0.003	0.009	0.006	/
Cutoff Frequency (Hz)	527	548	513	487	445	790	660	**567**

Figure 44: Table of Values for Reverberation Chamber

Reverberation Chamber							
Center Frequency 1/3 Octave Bands (Hz)							
	630	800	1000	1250	1600	2000	2500
R(ω) [m^2]	0.50	0.86	0.67	0.81	0.75	0.72	0.90
ᾱ(ω)	0.05	0.09	0.07	0.08	0.08	0.07	0.09
T60 [seconds]	0.59	0.34	0.44	0.36	0.39	0.41	0.32

4.3 Uniform Pressure Evaluation (Reverberation Chamber)

These tests were done in order evaluate the diffuse field within the reverberation chamber and to determine whether or not diffusers are necessary in the reverberant chamber for purposes of this device. Figure 45 shows a contour plot of the total sound pressure distribution on the panel. It is important to have a uniform pressure distribution across the panel and Figure 46 shows the deviation from the average across the panel. The largest deviation is 3dB. This is a

fairly large deviation and is isolated to one particular point. After observing the mounting for the sample it was determined that the deviation for that microphone was because of the sample mounting. The shape of the mounting caused extra reflection on that portion of the panel and was altered in order to correct that deviation.

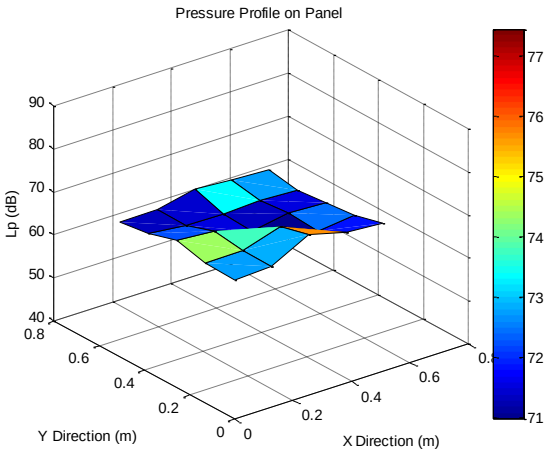

Figure 45: Total Sound Pressure Profile on Panel

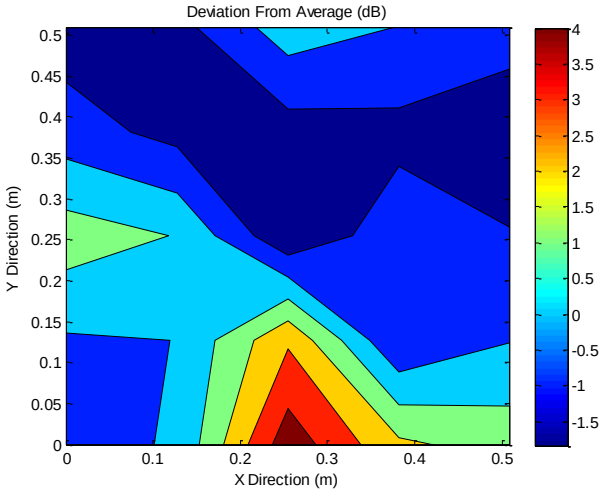

Figure 46: Deviation from Average Pressure on Panel

Figures 47 and 48 show frequency spectrum for 1/3 octave bands for all 25 microphones; again this data looks very uniform one exception, the same microphone discussed previously. Figure 47 includes data below the cutoff frequency to illustrate why the cutoff frequency is so important to data collection. Data below the cutoff frequency is very erratic and should not be considered in analysis.

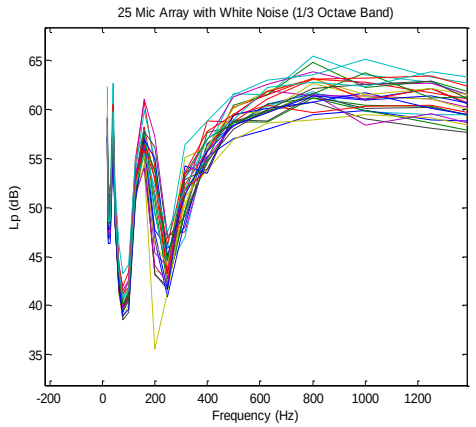

Figure 48: 25 Microphone Array 1/3 Octave Band Frequency Spectrum Near Cutoff Frequency

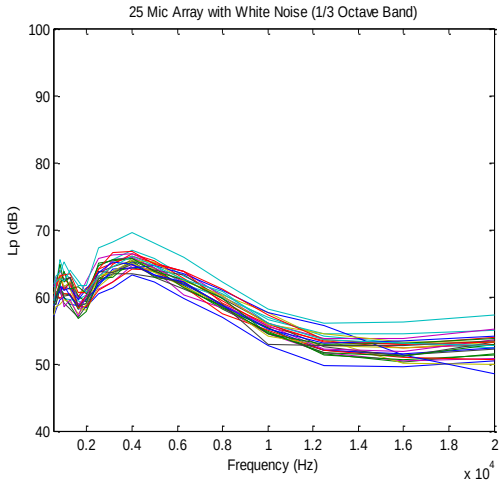

Figure 47: 1/3 Octave Band Frequency Spectrum for all 25 Microphones

Similar plots are shown by Figures 49 and 50 for data taken at various points in the room. Again Figure 49 illustrates the data near the cutoff frequency and Figure 50 shows very similar distributions for various points in the room. Figure 51 shows a table of the total sound pressures found at various points in the room. Deviation of +/-1 dB can be dismissed as insignificant deviation; the maximum value of deviation in this field is 1.43 dB which is very low. [1] Therefore, it can be assumed that this is a diffuse field for purposes of this project and no diffusers are needed for this frequency range.

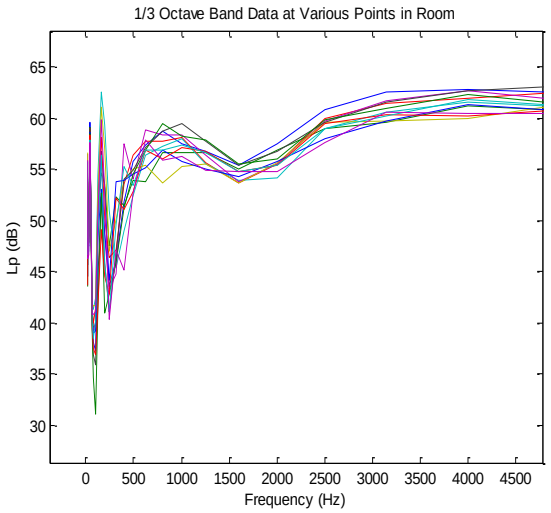

Figure 49: 1/3 Octave Band Frequency Spectrum Near Cutoff Frequency for Various Points in the Room

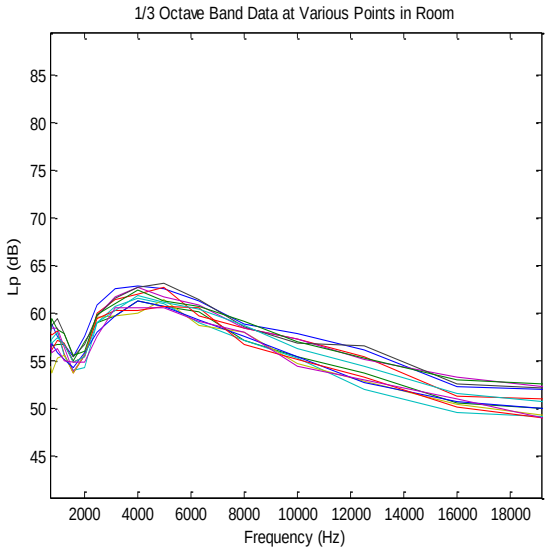

Figure 50: 1/3 Octave Band Frequency Spectrum for Various Points in the Room

Figure 51: Table of Total Sound Pressure Levels at Various Points in the reverberant Chamber

Mic Placement				
x (m)	y (m)	z (m)	Lp (dB)	Deviation From Average (dB)
0.46	0.30	0.46	70.2	**0.36**
0.76	0.30	0.46	68.6	**-1.23**
0.46	0.61	0.46	70.5	**0.70**
0.76	0.61	0.46	68.4	**-1.43**
0.46	0.91	0.46	70.5	**0.74**
0.76	0.91	0.46	69.0	**-0.77**
0.46	0.30	0.91	70.8	**1.03**
0.76	0.30	0.91	70.8	**0.99**
0.46	0.61	0.91	70.3	**0.45**
0.76	0.61	0.91	68.9	**-0.94**
0.46	0.91	0.91	69.9	**0.09**

4.4 Transmission Loss Measurements

Figure 52 reports the noise reduction from the room to the outside air. Values range from 27-40 dB which indicates that the chamber is well sealed from ambient sound.

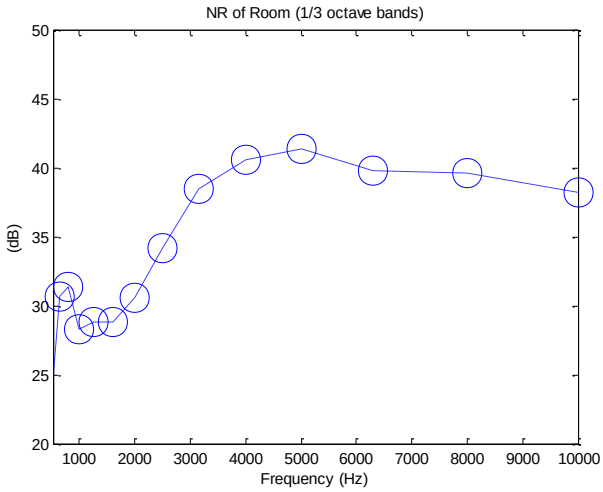

Figure 52: Noise Reduction of Room (to Outside)

Figure 53 and the table in Figure 54 show TL values for varying air gaps. The table also provides values of IL, and NR for reference. As expected, not much difference in TL was noticeable until a .2% gap was added to the panel. Comparing these values to the theoretical values from Figure 55, they are very close predicted values. [14]

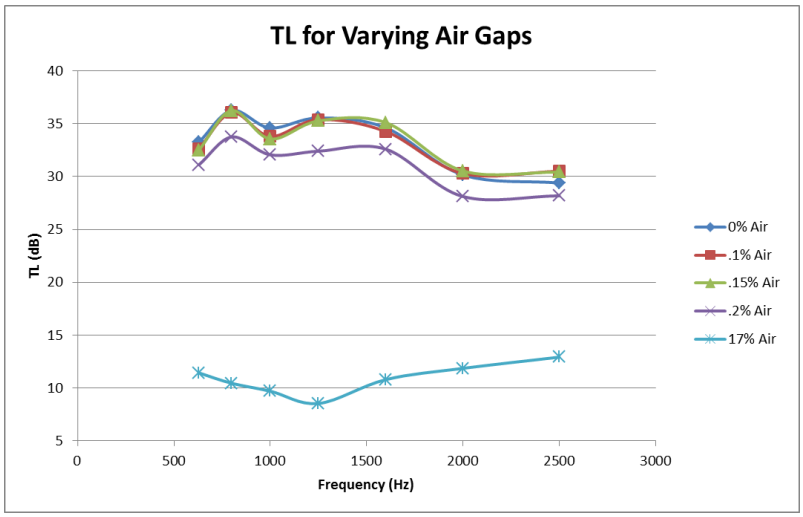

Figure 53: Plot of TL at Varying Air Gaps

Figure 54: Table of TL, IL, and NR for Varying Air Gaps

Center Frequency 1/3 Octave Bands (Hz)								
% of air		630	800	1000	1250	1600	2000	2500
0.00	TL	33	36	35	36	35	30	29
	IL	20	23	22	25	22	17	15
	NR	39	42	41	42	41	36	35
0.1	TL	33	36	34	35	34	30	31
	IL	19	23	22	24	21	17	16
	NR	39	42	40	41	40	36	37
0.15	TL	33	36	34	35	35	31	30
	IL	19	23	22	24	22	17	16
	NR	39	42	40	41	41	37	36
0.2	TL	31	34	32	32	33	28	28
	IL	18	21	21	22	20	16	14
	NR	37	40	38	38	39	34	34
17	TL	11	10	10	9	11	12	13
	IL	N/A	N/A	N/A	N/A	N/A	N/A	N/A
	NR	17	16	16	15	17	18	19

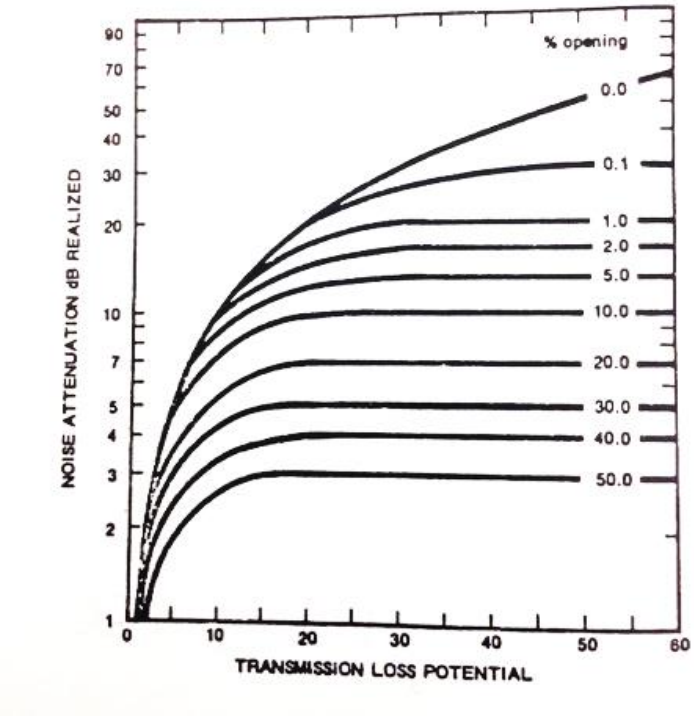

Figure 55: TL Potential for % Air Opening [14]

Given TL potential of 35 dB the TL values for a 17% opening should be around 8 dB and they are mostly around 10 dB. Figure 56 shows a table comparing the theoretical and measured values of realized transmission loss at 1250 Hz. Figure 57 shows plots of theoretical and measured values over a wider frequency range.

Figure 56: Table of TL Data at 1250 Hz

TL Data for 1/3 Octave Band Centered at 1250 Hz			
% of Air	**TL Potential [dB]**	**TL Realized (Measured) [dB]**	**TL Realized (Theoretical) [dB]**
0.1	36	35	30
0.15	36	35	28
0.2	36	32	26
17	36	9	7

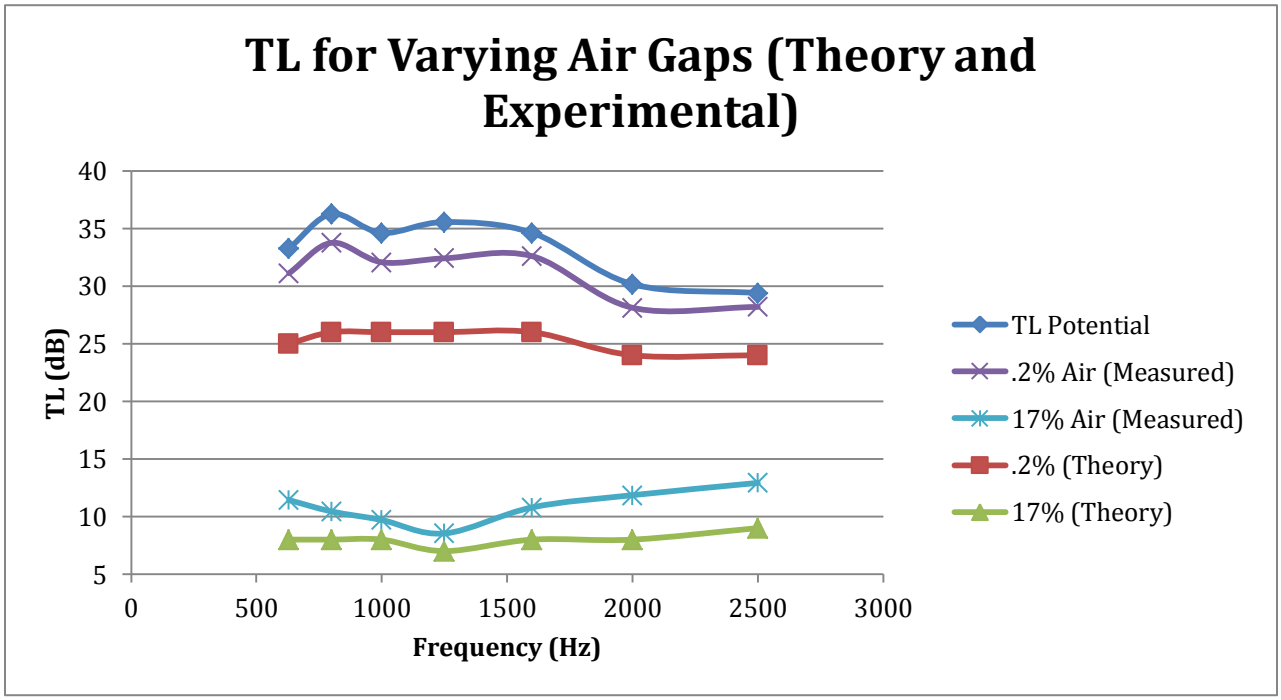

Figure 57: Comparing Theoretical and Experimental TL

Chapter 5: Conclusions

5.1 Conclusion

The main objective of this project was to develop a test to characterize random incidence properties of acoustic materials. By reviewing ASTM standards it was determined that a split chamber design would be the best solution for this project. Given sizing and budgetary constraints at target cutoff frequency of 500 Hz was chosen. The design process included several iterations but the final chamber was very similar to the final design. This chamber was built to be within the sizing constraints and under budget. Evaluation of this chamber yielded a cutoff frequency of approximately 570 Hz which is above the target, however it is very reasonable considering the constraints and the purposes of this chamber. The theoretical calculations consisted of both field theory and surface interaction. A great deal of time was spent characterizing the field within each room; this is a valuable concept to understand and to have experience with considering that the purpose of this chamber is to characterize materials that treat such rooms of varying contributions from the direct and diffuse fields.

Values of $R(\omega), \bar{\alpha}(\omega),$ & T_{60} were determined for both anechoic and reverberant rooms. The anechoic chamber yielded $\bar{\alpha}(\omega)$ values ranging from .78 to .9 and reverberation times ranging from .003 seconds to .008 seconds. These values are quite reasonable considering that the anechoic chamber in this design could nearly be considered hemi-anechoic because of the large amount of surface area not treated (the sample size). The slope for sound pressures at varying distances from the source was found to be -5.7 dB/octave which is very close to the -6 dB/octave theoretical value. The reverberant chamber yielded $\bar{\alpha}(\omega)$ values ranging from .05 to .09 and reverberation times from .32 seconds to .59 seconds. This values fall within reasonably

expected values. When total sound pressures were analyzed in a 25 microphone array on the panel there was hardly any deviation except for one point; this deviation was a result of the mounting. When the diffuse field was evaluated by taking total sound pressure measurements it was determined that the pressure in the room was sufficiently uniform and no diffusers were needed.

TL data was collected for the room itself and it was determined that the room was well sealed and there is no need for further insulation. When TL data was collected for varying air gaps measured results yielded values very close to theoretical. With a 17% opening there was a TL of 10 dB realized when theoretical values were near 7 dB. The main objective of the project was completed; there is now a test chamber and a test method for determining $\bar{\alpha}, TL, \& IL$ values for acoustic materials. This chamber was never intended to meet the ASTM standards but will serve as a valuable tool for the Acoustic and Dynamics Laboratory and for future educational purposes in Mechanical Engineering coursework. Those classes include ME 8260 (Advanced Acoustics) and the Auto NVH sequence.

5.2 Sources of Error

Acoustic experimental measurements measure very small pressure perturbations from equilibrium. It is extremely difficult to report these measurements within a high degree of accuracy, thus there are several sources within any acoustic testing set-up that might cause error. Faulty equipment; microphones, cable, data acquisition systems, etc. can cause significant error if not properly calibrated. However, most measurements for this project were relative measurements and microphones had been previously calibrated. A simple yet significant source of error would be distance measurements. Distance measurements such as room size and distance

from the source were taken with a standard tape measure and can only provide accuracy to the nearest 5 mm. The biggest source of error from these experiments would be structural borne noise. Sound sources often have both airborne and structural borne noise components and all measurements and calculations assumed only airborne noise. Structural borne noise would come from the sound source (either known power source or the speakers) exciting the enclosure walls to which it is attached. This structural borne noise would increase all of the sound pressure values; which is less important for relative measurements but would result in higher values for absorption. Ways to improve this error would be to add more dampening to the structure; this could be done by applying mass loaded vinyl (MLV) to the sample mounting brackets and to the mounting for the sound sources. MLV or other vibration absorbers could be added to the outside of enclosure walls to reduce structure borne vibrations.

5.3 Recommendations for Future work

The design itself turned out just as expected but I would change a few things to increase the accuracy of the chamber. Firstly, large acoustic wedges should be added to the anechoic side. The reasoning for buying 6" of acoustic material was because of budgetary constraints. In order to maximize performance another $500 would be necessary to increase the amount of foam to 12". Future work would also include exploring the possibility of using diffusers in the reverberant chamber. As part of my ME 8260 coursework I will analyze the effects of diffusers with boundary element software (Coustyx) and compare this with experimental results.

This chamber can be used for the purpose defined in section 3.5; however, this test chamber can also be altered to serve as an anechoic test chamber. By simply adding a wire grid to cover the bottom foam wedges, objects could be placed in the room for testing. Also, future

work might include developing laboratory exercises for the various classes involving acoustics. This would also involve promoting the use of the chamber.

Appendix

Bill Of Materials			
Part	**Quantity**	**Source**	**Cost ($)**
8'x4' MDF Pieces	6	Lowes	220
Clamps	4	McMaster-Carr	60
Casters	8	McMaster-Carr	80
2" foam (80"x72" sheet)	2	The Foam Factory	150
4" foam (2'x4' sheet)	12	The Foam Factory	230
1/4"x1" Foam Sealant	16 ft	Lowes	20
1/2"x3/4" Foam Sealant	16 ft	Lowes	20
Foam Adhesive Tube	6	Lowes	30
Bathroom Chaulking Tube	1	Lowes	4
Drywall screws	300	Lowes	6
Mounting Brackets	32	Lowes	6
5/16" Through Bolts	120	Lowes	5
5/16 " Nuts	120	Lowes	5
Wsahers	120	Lowes	5
		Total Cost=	**841**

First Design Sketch

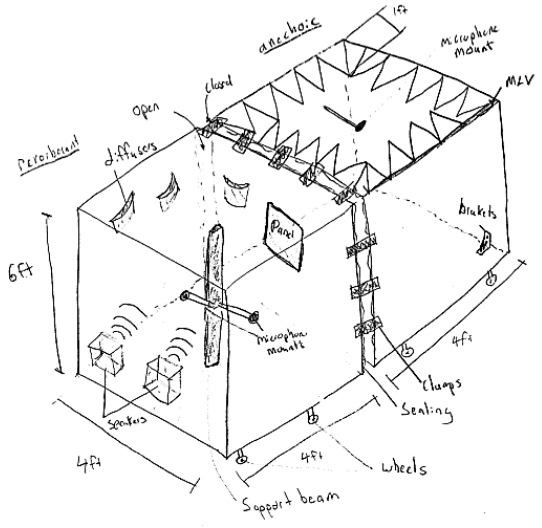

List of Symbols Used

dB=Decibels

Hz=Hertz

TL= Transmission Loss

IL=Insertion Loss

NR=Noise Reduction

α=absorption coefficient

$\bar{\alpha}$=average absorption coefficient

$\emptyset_i$=angle of incident sound

$\emptyset_r$=angle of reflected sound

λ=wavelength

ε_d = energy density

T_{60} = Reverberation time

z=acoustic impedance

p=pressure

u=particle velocity

$\widetilde{z_s}$=specific impedance

L_p = Sound pressure level (dB)

Γ=Directivity of sound source

f_n=fundamental frequency

n=Integer

S=Surface area

$sabine'$s=dimensionless unit assigned to absorption

$R(\omega)$=Room constant at given frequency ω

L_w=Sound power

f_c=cutoff frequency

c_o=speed of sound in air

p_o=Density of air

I_i=Incident sound intensity

V_n^2=Variance

N=number of samples

$< P_{rms}^2 >_t$=Root mean square pressure

References

[1] Lord, Harold W., William S. Gatley, and Harold A. Evensen. *Noise Control For Engineers*. Malabar: Krieger, 1980.

[2] ASTM E90, "Standard Test Method for Laboratory Measurement of Airborne Sound Transmission Loss of Building Partitions and Elements." ASTM International, West Conshohocken, PA, 2009.

[3] ASTM C423, "Standard Test Method for Sound Absorption and Sound Absorption coefficient by the Reverberation Room Method." ASTM International, West Conshohocken, PA, 2009.

[4] Everest, Alton F. *Master Handbook of Acoustics*. Fifth ed. New York: Mc Graw Hill, 2009.

[5] A. Kahraman, "MechEng 5240 Engineering Acoustics" Spring 2013

[6] R. Singh, "ME 8260 Course Notes *Advanced Engineering Acoustics*" SP 2013 Edition

[7] Bruel &Kjaer, *Measurements in Building Acoustic.* 1988*s*

[8] Pierce, Allan D. *Acoustics: An Introduction to Its Physical Principles and Applications*. New Zealand: Mc Graw Hill, 1989..

[9] Reference sound source. Manufacturer: ILG Industries, Inc., 2826 North Pulaki Road, Chicago, Ill. 60641.

[10] "Acoustic Test Chambers." | *ETS-Lindgren*. N.p., n.d. Web. 12 Mar. 2013.

[11] ASTM C384, "Standard Test Method for Impedence and Absorption of Acoustic Masterials by Impedence Tube Method." ASTM International, West Conshohocken, PA, 2009.

[12] "Performance Testing." *Architectural Testing:*. N.p., n.d. Web. 12 Mar. 2013

[13] "McMaster-Carr." *McMaster-Carr*. N.p., n.d. Web. 12 Mar. 2013.

[14] Rao, Mohan D., and Harold A. Evensen. *Supplemental Notes to Acoustics and Noise Control*. N.p.: Michigan Tech University, n.d. Print.